SURFACE INTEGRITY AND TRIBOLOGICAL BEHAVIOUR OF HARDENED STEELS

ZDENEK PALA[a], NIKOLAJ GANEV[b], KAMIL KOLAŘÍK[c], OLGA BLÁHOVÁ[d], and JAN JERSÁK[e]

[a] Department of solid state engineering, FNSPE, CTU in Prague, Trojanova 13, 120 00 Prague, [b] Department of solid state engineering, FNSPE, CTU in Prague, Trojanova 13, 120 00 Prague, [c] Department of solid state engineering, FNSPE, CTU in Prague, Trojanova 13, 120 00 Prague, [d] Department of mechanics, Faculty of applied sciences, University of West Bohemia, Univerzitní 22, 306 14 Pilsen, [e] Department of machining and assembly, Faculty of mechanical engineering, Technical University of Liberec, Studentská 2, 461 17 Liberec , Czech Republic
zdenek.pala@fjfi.cvut.cz, nikolaj.ganev@fjfi.cvut.cz, kamil.kolarik@fjfi.cvut.cz, blahova@kme.zcu.cz, jan.jersak@vslib.cz

Keywords: residual stresses, milling, friction, surface roughness

1. Introduction

Crystal structure undoubtedly belongs to the crucial factors influencing the local mechanical properties of a solid body. Yet perfect crystals are virtually nonexistent[1] and, hence, defects are a common matter. When a polycrystalline material is considered, such "crystallographic factors" as grain size and grain boundaries must be taken into account. Moreover, internal or residual stresses are often present. Occurrence of these stresses is facilitated by processes of inhomogeneous plastic deformation and/or by the presence and temporal evolution of thermal fields and/or the existence of phase transformations[2]. However, residual stresses have rarely been taken into account when mechanical properties, wear and friction are studied, and traditionally only microstructure, surface morphology, microhardness and roughness represent the group of investigated parameters.

The surface area of a solid body is extremely important and its qualities are paramount for numerous applications. It is often a challenge to choose the magnitudes that would serve best to assess the suitability of the surface for its putative usage. The last decade has seen the term surface integrity[3] in the crosshairs of material science. It encompasses not only traditional surface characteristics, but also more novel ones such as macroscopic and microscopic residual stresses, grain size, texture and dislocation density. The aim of the introduction of a new set of characteristics was to improve understanding of the role played by surface structure and microstructure in which they determine above all the mechanical properties and preordain the future behaviour of the whole body in a given environment.

It would be especially beneficial to establish the mutual relationship between surface integrity on one hand and wear and friction on the other. This would facilitate the optimisation of surface treatment processes leading to improved fatigue and longer service life. Nevertheless, the direct, general and even qualitative links mentioned above are lacking and, according to some material scientists[4], may be boldly rendered as only wishful thinking. Yet there have been attempts[5] to elucidate such links for certain type of material structure with a given real structure, i.e. deviations from the perfect structure of ideally crystalline material which covers diverse areas ranging from macroscopic parameters to nano-scopic ones.

In our contribution, we strive to analyse the surface by means of four surface integrity parameters, i.e. macroscopic and microscopic residual stresses, roughness and microhardness, and compare them with the results of tribological investigations. This research has not only academic purposes, but also serves as vital information for decision making by our industrial partner when the most appropriate tool tips for implementation in its horizontal milling machine have to be selected.

2. Experimental

2.1. Samples

The surface layers of three pairs of samples were investigated. The samples were in the form of two parts of guide gibs from steel ČSN 14100.3 (59 – 61 HRC) embedded into a cast iron bed (ČSN 422425). These samples were subjected to side milling by tool tips produced by three manufacturers and marked as *SA2*, *SA3*, *SE2*, *SE3*, *WA2*, and *WA3*. Table I shows the working and cutting parameters of applied milling where a_p [mm] is depth of cut, n – number of cuts, d [min] – tool´s diameter, f [mm min^{-1}] – shift, v_c [m min^{-1}] is cutting speed, and f_z [mm] – feed per tooth.

Table I
Working and cutting conditions for investigated surfaces

Sample	a_p	n	d	f	v_c	f_z
SA2	0.5	4	100	570	300	0.10
SA3	0.3	7				
SE2	0.5	3	63	1050	350	0.10
SE3	0.3	7				
WA2	0.5	3	160	500	60	0.17
WA3	0.3	7				

2.2. X-ray diffraction

Macroscopic and microscopic residual stress data were furnished by X-ray diffraction which is acknowledged to be a suitable and accurate tool. The measurements were performed on a θ/θ goniometer X´Pert PRO with *CrKα* radiation.

The diffraction line {*211*} of *α-Fe* phase was analysed. The ***sin²ψ*** method [6] with nine different tilt angles ψ was used. The X-ray elastic constants $½s_2 = 5.76 \cdot 10^{-6}$ MPa^{-1}, $-s_1 = 1.25 \cdot 10^{-6}$ MPa^{-1} were used in macroscopic stress calculations of biaxial state. The single line Voigt function method[7] was applied for corrections of instrumental broadening and the determination of microstrains and particle size. The microstress σ^{micro} could be calculated from the microstrains e using Hooke's law ($\sigma = e\,E$) with the Young modulus E = 216 GPa in order to be comparable with macroscopic residual stress.

2.3. Hardness and roughness measurements

The measurements were made on a *Buehler MICROMET 2100* microhardness tester with a 200 g load, which was assessed as the optimal load with regard to indentation readability from all the investigated surfaces.

Surface roughness was analysed using a *MITUTOYO SURFTEST 2000* contact profilometer. A trace 4.0 mm long was evaluated with cut off length of 0.8 mm to obtain surface roughness data.

2.4. Tribology measurements

In order to analyse friction and wear, the pin-on-disc test was used. During this test, the coefficient of friction was continuously monitored as wear occured; material removal was determined by weighing and measuring the profile of the resulting wear track. The operating conditions were set to simulate, as precisely as possible, those in a working process.

The measurement of friction coefficient was undertaken using a *CSM High Temperature Tribometer*. The specimens' surfaces after the pin-on-disc test were observed by light microscopy and scanning electron microscopy.

The friction tests were performed with two different layouts (Fig. 1) using a "polymer"cylinder with diameter 5.5 mm. The tests were carried out using a 2 N constant load and a linear relative speed dependent on radius of track (speed = radius/2). In the first case, the cylinder and the weight holder formed an angle of 45° in the plane formed by the axis of the holder and the sensing arm (Fig. 1, left). In the second case, the cylinder and the weight holder formed an angle of 45° in the plane perpendicular to the plane formed by the axis of the holder and the sensing arm (Fig. 1, right). The wear test was performed with 5,000 laps at room temperature.

3. Results

The obtained surface integrity characteristics are summarised in Table II. The values of macroscopic residual stress along the cut's shift direction σ_L, perpedicular cut's shift direction σ_T, microstrains ε_{micro} and surface roughness *Ra* are averages from measurements in three areas chosen on the investigated surfaces. The hardness *HV0.2* is a mean value from 18 locations on the analysed surface.

The experimental error of macroscopic residual stress´ measurements $\Delta\sigma$ does not exceed 20 MPa, $\Delta\varepsilon_{micro} < 3 \cdot 10^{-4}$, and the 95 % confident interval of *HV0.2* is smaller than 1 % of the values below.

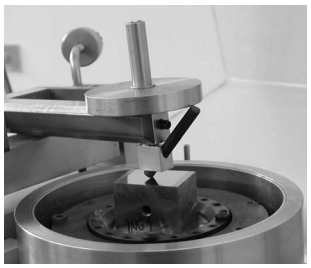

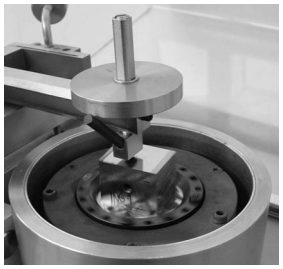

Fig. 1. **Pin-on-disc test layout**

Table II
Results of surface integrity parameters on the measured surfaces

Sample	σ_L [MPa]	σ_T [MPa]	ε_{micro} [$\times 10^{-4}$]	*Ra* [μm]	*HV0.2*
SA2	– 113	– 137	29.7	0.23	769
SA3	– 150	– 179	28.4	0.22	762
SE2	– 353	– 125	24.7	0.09	762
SE3	+ 31	+ 311	30.4	0.14	758
WA2	– 451	– 520	35.9	0.75	835
WA3	– 390	– 395	36.7	0.71	818

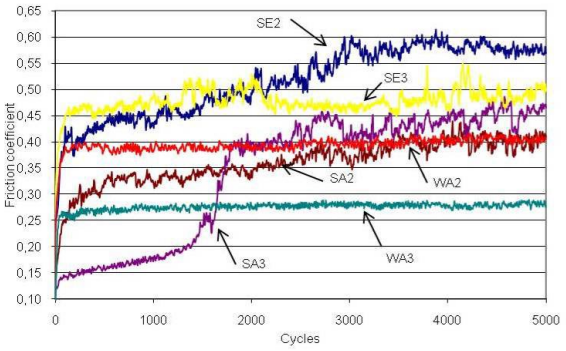

Fig. 2. **Friction coefficient curves for layout 1**

Comparisons of friction coefficient curves at different radii for all samples are in Figs. 2 and 3.

4. Discussion

It has been shown[8] that, in general, compressive residual stresses can favourably reinforce dynamic strength by about 50 %; on the other hand, tensile stresses could reduce the dynamic strength by about 30 %. The advantageous effect can be derived from a mechanical model of counterbalancing, when residual stresses mitigate the adverse effects of tensile load stresses[9] that occur during the lifetime. The concept of

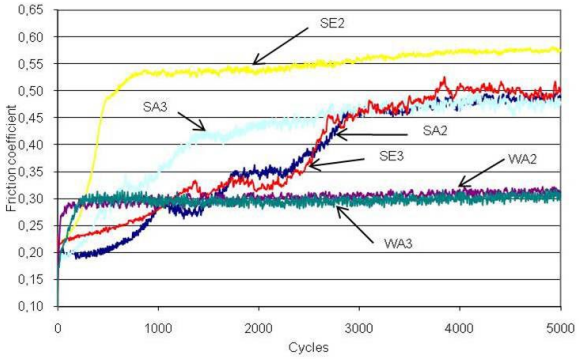

Fig. 3. **Friction coefficient curves for layout 2**

compressive stresses as an elastically compressed lattice would also explain their beneficial role in corrosion resistance.

In the studied case, favourable compressive macroscopic stresses were obtained on all the samples with the exception of surface *SE3*, where tensile residual stresses were found. At the same time, this sample showed significant anisotropy and $\sigma_T = 10\ \sigma_L$. As can be seen from Tab. I & II, only in the case of the tool *SE* is surface residual stress very sensitive to the cutting depth a_p, i.e. when a_p changed from 0.5 mm to 0.3 mm compressive RS of – 353 MPa converts to tensile RS of + 31 MPa. These observations could be explained by the small tool diameter and big shift resulting in a cutting forces' distribution different from the case of *SA* and *WA* tools.

The *WA* tools generate the highest compressive residual stresses and the biggest values of microhardness and microstrains. These facts give evidence of a predominant effect of inhomogeneous plastic deformation of surface layers during cutting in comparison to thermal influence, which is apparently a consequence of the (5–6 times) slower cutting speed and the (4 times) greater number of teeth with respect to the remaining two tools.

In the case of side milling, surface microrelief is a result of the tool's revolving and relative feed of the tool and a workpiece, and thus depends on the measuring direction. The values *Ra* in Tab. II are obtained in the direction of cut's shift (σ_L). As can be seen from Tab. II, the depth of cut does not have any impact on the surface roughness and *Ra* primarily depends on the tool's diameter, its feed and cutting speed.

The obtained average surface hardness of 770–860 HV0.2 corresponds to the values expected for the hardened 14100 steel. This demonstrates that no additional hardening took place as a result of plastic deformation during machining. The temperature on the surface increases with increasing cutting speed, which leads to a microhardness decrease (see Tab. II) of the technologically influenced subsurface layer. In all the investigated cases, deeper cuts (a_p = 0.5 mm) lead to slightly higher microhardness HV0.2 in comparison to a_p = 0.3 mm, even though the differences are within the experimental precision.

Although the values of tribology test parameters are higher than the operational ones for components in contact, the specimen material (steel) showed no damage. The material from the cylinder (polymer) was transferred onto the steel surface in all tests, but the most visible wear traces were on *WA* samples.

Samples *WA2* and *WA3* showed the highest surface roughness, i.e. more than 0.7 μm *Ra*, along with the most uniform or less scattered friction coefficients curves in both layouts. According to Tab. I, these two samples are distinguished by the highest compressive residual stresses.

It is worth emphasising that the highest friction coefficient was obtained for *SE* samples with the lowest roughness while the lowest friction coefficient for *WA* samples with the highest roughness.

Pondering the differences between the two tribology test layouts used, the lower scatter of friction coefficient was determined for layout no. 2.

5. Conclusions

The performed analyses facilitate drawing these main conlusions:

- The surfaces of all analysed samples are homogeneous from the point of view of studied surface integrity characteristics.
- The high roughness in *WA* surfaces does not negatively influence friction coefficient. In a similar matter, low roughness (*SE*) leads to high friction coefficient.
- The best, i.e. the lowest, scatter of friction coefficient curves was recorded on surfaces with the highest roughness (*WA*).
- The lowest friction coefficients were found in surfaces milled with the *WA* tool that, at the same time, is distinguished by the highest compressive residual stresses.
- Increasing cutting speed leads to a rise in temperature at the cutting zone which results in a decrease of measured microhardness.
- The change of the cutting depth from 0.3 to 0.5 mm does not have any impact on the surface roughness values.

The research was supported by Project № 101/09/0702 of the Czech Science Foundation and by Project MSM 6840770021 of the Ministry of Education, Youth and Sports of the Czech Republic.

REFERENCES

1. Welzel U., Ligot J., Lamparter P., et al.: J. Appl. Cryst. *38*, 1 (2005).
2. Mahdi M., Zhang L. C.: J. Mater. Process. Technol. *95*, 238 (1999).
3. Leskovar P., Peklenik J.: CIRP Anals – Man. Tech. *31*, 447 (1982).
4. Persson B. N. J.: *Sliding Friction - Physical Principles and Applications*, Springer-Verlag, Berlin 1998.
5. Williams J.: *Engineering Tribology*, Cambridge University Press, New York 2005.
6. Hauk V. et al.: *Structural and Residual Stress Analysis by Nondestructive Methods*, Elsevier Science B. V., 1997.

7. de Keijser Th. H., Langford J. I., Mittemeijer E. J., Vogels A. B. P.: J. Appl. Cryst. *15*, 308 (1982).
8. Youtsos A. G.: *Residual stress and its effect on fracture and fatigue*, Springer 2006.
9. Abu-Nabah B. A., Nagy P. B.: NDT&E International *40*, 405 (2007).

Z. Pala[a], N. Ganev[b], K. Kolařík[c], O. Bláhová[d], and J. Jersák[e] *([a] Department of solid state engineering, FNSPE, CTU in Prague, [b] Department of solid state engineering, FNSPE, CTU in Prague, [c] Department of solid state engineering, FNSPE, CTU in Prague, [d] Department of mechanics, Faculty of applied sciences, University of West Bohemia, [e] Department of machining and assembly, Faculty of mechanical engineering, Technical University of Liberec):* **Surface Integrity and Tribological Behaviour of Hardened Steel.**

A comparison between the results of tribological investigations and four surface integrity parameters, i.e. macroscopic and microscopic residual stresses, roughness and microhardness, was performed. The samples in the form of two parts of guide gibs from steel embedded into a cast iron bed were subjected to side milling by three different tool tips. The performed analysis yields some mutual relationships between surface integrity and friction coefficient, e.g. low roughness lead to high friction coefficient, the highest compressive residual stresses were found for the lowest friction coefficients, or increasing cutting speed leads to a decrease in microhardness.

EFFECT OF INDICATION LIQUIDS ON BRITTLE-FRACTURE PROPERTIES OF VITREOUS ENAMEL COATING

KAMILA HRABOVSKÁ[a]*, JITKA PODJUKLOVÁ[b], ONDŘEJ ŽIVOTSKÝ[a], KARLA BARČOVÁ[a], IVO ŠTĚPÁNEK[c], VRATISLAV BÁRTEK[b], and TOMÁŠ LANÍK[b]

[a] Institute of Physics, [b] Faculty of mechanical Engineering VŠB -Technical University of Ostrava, 17. listopadu 15, 708 33 Ostrava Poruba, [c] Faculty of mechanical Engineering, University of West Bohemia in Pilsen, Univerzitní 8, 306 14 Plzen, Czech Republic
kamila.hrabovska@vsb.cz

Keywords: vitreous enamel coating, steel, microhardness, mechanical properties, indication liquid

1. Introduction

Enamel coatings belong to the category of vitreous ceramic covering crusts providing very high resistance of steel substrates against damage and corrosion. This type of coatings can be used in energetic, environmental, or agricultural machinery, in architectonic design and civil engineering, in car industry, health service, and in products of consumer goods[1–6]. However, creating a compact enamel coatings without faults is the essential precondition for using its functional properties[2,3].

Undesirable faults of coatings may occur e.g. by selection of an unsuitable foundation substrate, type of enamel coat, or by the technological procedure of enamelling. One of the most serious problems is the hydrogen faults (fish scales) created by the hydrogen penetrating to the surface of the coat from the steel – enamel boundary[1].

Low voltage test (LVT) is usually performed to verify surface properties of the enamel coatings and to determine material defects (according to the ČSN EN ISO 8289 standard). The LVT test is realized using indication liquids (containing water, water-soluble salts and surfactant) as and electricaly conductive solutions. Unfortunately, the testing standard does not indicate any way of cleaning the coat from indication liquids. Long-time treatment of the indicating liquids after LVT testing may cause the damage of the surface layer and the creation of faults detected by customer´s acceptance test[7–13].

The main aim of this paper is to investigate the influence of indication liquids on brittle – fracture and mechanical properties of the under-coat and top-coat enamels. To realize this aim a number of modern experimental methods were applied (expecially scratch and nano-indentation test).

2. Sample preparation

For experimental testing, a steel plate was used as the substrate with the following properties: the quality of kosmalt E 300T (produced by U.S. Steel Košice) and the thickness of 3 mm (chemical composition (weight %): C: 0.041; Si: 0.02; S: 0.007; N: 0.006; Mn: 0.241; P: 0.010; Al: 0.052; Ti: 0.067; Cr: 0.023; Mo: 0.005; V: 0.005). The surface of hot-rolled steel plate was treated by mechanical shot blasting to obtain the surface cleanliness of Sa 2.5 (ČSN EN ISO 12944-4) and additionally degreased for 5 minutes in the degreasing alkali liquid Simple Green with the concentration of 1:10 and the concentrate pH of 9.4.

The 24 hour-old enamel slurry was applied on degreased steel substrate by pneumatic spraying, dried at the temperature of 100 °C for 5 minutes, and subsequently burned at the temperature of 820 °C for 8 minutes. Consequently the samples were cooled in air at the temperature of 20 °C. In accordance to the colour were distinguished two types of enamels: the grey (basic under-coat) and the green (top-coat). The consistence of both enamels is 1750 kg m^{-3} and main chemical composition (wt.%): 25 quartz ground, 8 clay MIC, 0.4 boric acid, 0.3 Sb_2O_3, 0.05 K_2CO_3, 0.15 $NaNO_2$ and 56 water. Undercoat enamel layer forms the function interlayer in enamel-metal system. Due to higher content of elements (Si, Ni, Ca, K …) it caused increasing adhesion of glassy phase to the substrate and strongly influences a surface design of final product[14–19].

Surface properties of three different samples were investigated. Sample 1 is the initial degreased steel substrate covering by grey under-coat and green top-coat enamel layers without the exposure of any indication liquids. Sample 2 containes the same enamel layers as sample 1, but the surface was additionally treated by the NaCl indication liquid (30 g NaCl per 1 l water + liquid tenside). Surface treatment of the sample 3 was performed using $NaNO_2$ indication liquid (30 g $NaNO_2$ per 1 l water + liquid tenside). Average electrical conductivities of NaCl and $NaNO_2$ enriched liquids were determined to 50.858 mS and 50.231 mS with pH of 8.02 and 8.19. Such prepared samples were waterproofly packed according to the storage prescripts of manufacturing, time of exposure of indication liquids was chosen for 3 weeks at the laboratory temperature of 20 °C. This time period represents the usual time interval between the production output check of the enamel coat and the customer's acceptance of the product. The thickness of both layers of enamel coating (under-coat and top-coat) is 200 μm.

3. Experimental methods

Microhardness measurements and fracture toughness

Microhardness is defined as a resistance of material to local plastic deformation, which is established by the loading of surface by an indenter. To determine the H_V parameter describing the microhardness using the Vickers method was used Hanemann microhardness tester (NEOPHOT 2 optical microscope) with a diamond pyramid indenter with the apex angle of 136°. Indenter was impressed perpendicularly to the surface of investigated coat with the force of 1 N during the

time of 10 s (ref.[14–19]).

Using microhardness measurements were defined critical values of the stress intensity coeficient K_Ic for investigated samples. At this value of stress intensity the crack does not propagate. Fracture toughness is an indication of the amount of stress required to propagate a preexisting flaw. It is a very important material property since the occurrence of flaws is not completely avoidable in the processing, fabrication, or service of a material/component. Flaws may appear as cracks. On the basic of the resultant values microhardness and Palmquist crack length (Fig. 1) we determined the fracture toughness K_Ic (equation (*1*)).

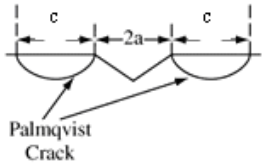

Fig. 1. **Palmqvist Crack formation by Vickers indentation**

Palmqvist crack formula used for the evalution of the fracture toughness[14]:

$$K_{IC} = 0.035\left(\frac{c}{a}\right)^{-\frac{1}{2}}\left(\frac{Ek}{H_v}\right)^{\frac{2}{5}}\left(\frac{H_v a^{\frac{1}{2}}}{k}\right) \qquad (1)$$

for:

$$0{,}25 < \frac{c}{a} < 1{,}5$$

E – Young modulus, H_v – microhardness, a – half diagonal length of the microindentation, k – constraint factor ≈ 3, c – total crack length.

Resistance to shot (shot firing test) and abrasion (by ball tester)

Shot firing tests were provided using steel ball with diameter of 5 mm fired towards on enamel surface with the increasing impact force in the range 10–90 N. Adhesion of vitreous enamel coating was obtained according to the Wegner instrument in compliance with ČSN ISO 4532 (945050) standard.

A rotating steel ball with diameter of 30 mm affecting a certain place of the enamel coat surface was used for test checking the resistance to abrasion.

Surface roughness

ČSN ISO 4287 standard was used for evaluation of the surface roughness. Coating roughness (as a deviation with the rexpect to the mean line of the profile) is defined by 2 main parameters: Ra – mean arithmetic deviation of the profile and Rz – miximum height of the profile. Our measurements were performed using the contact profilometer Mitutoyo, SurfTest SJ-301 with mobile measurement head fitted by a retractable diamond stylus sensor (5 μm/0,2 mils radius) and working at load of 4 mN.

Scratch, static and nano indentation test

A scratch indentation test was carried out by means of a diamond indenter of the Rockwell type (cone) with the apex angle of 120° and radius of curvature of 0.5 mm. The value of normal loading affecting the indenter was changing with constant speed and the table with the fixed sample under the indenter was moving with the same speed as well. The range of normal force from 40 N to 80 N was used for the evaluation.

During the measuring process, the course of an acoustic emission signal depending on the acting of normal force was recorded. However, signals of the acoustic emission follow the deformation and fracture processes and provide integral information on the current dynamic state of material. After finishing the scratch test, we documented the morphology of failures with the help of a light microscope with highlighting of the failure by means of polarization and the Nomarsky differential contrast. Existence of brittle fractures was confirmed at the scratch indentation test and experimental analysis of the acoustic emission signal without sample moving (static indentation test). These surface-sensitive methods enabled to obtain the dependence of acting loading as a function of penetrating depth of the enamel. This experiment was done by means of the Nanoindenter SHIMADZU DUH – 202, the device with the following parameters: – indenter loading: 0.01–200 g (with the accuracy of 0.002 g), – depth of indentor penetration: 0–10 μm (with the accuracy of 0.001 μm).

3. Results and discussions

Differences between the surface structure of the initial steel plates before and after degreasing process are shown in Fig. 2. The as-prepared non-degreased plate exhibits dirty surface with the crack-type faults. The uniformity of shot blasting process proved positively influence of the adhesion to the vitreous enamel coating for degreased sample.

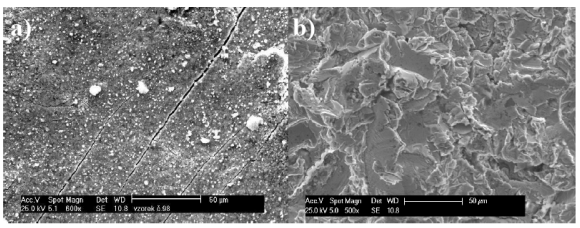

Fig. 2. **SEM analysis of the a) non-degreased and b) degreased, shot blasted raw steel plate surface**

Chemical element analysis and SEM micrographs of enamel slurries are compared in Tab. I and Fig. 3.

Experimental results clearly confirmed negative influence of indication liquids exposure on brittle-fracture properties of vitreous enamel coatings. Table II shows that sample 2 and sample 3 parameters of microhardness, fracture toughness, roughness of the coat and its adhesion are markedly deteriorated in comparison to reference sample 1. In the case of microhardness test the microscopic analysis showed in Fig. 4 indicate a visible damage of the surface, microcracks and conchoidal fractures with numerous Wallner lines ob-

Table I
Chemical analysis of the enamel slurry of grey basic enamel and green top enamel

Chemical element	grey under-coat	green top- coat
	total weight percentage Wt [%]	total weight percentage Wt [%]
O	32,76	29,57
Na	9,96	10,14
Al	6,05	7,26
Si	38,96	34,32
K	1,92	0,41
Ca	5,49	3,24
Ti	1,12	3,26
Fe	2,15	2,48
Co	0,46	2,63
Ni	1,13	-
Cr	-	6,68
Total	100	100

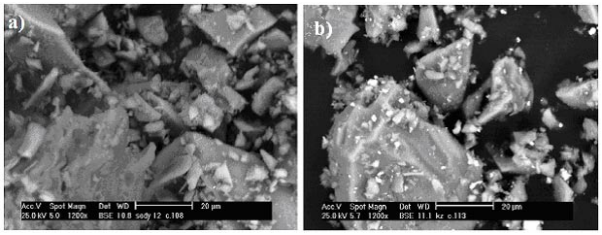

Fig. 3. **SEM analysis of the enamel slurry of grey basic enamel (a) and green top enamel (b)**

served in the neighbourhood of diagonals originated after the impress of Hanemann indenter. Such fractures are typical for brittle vitreous materials with low fracture toughness. In diagonals of an indenter impression the presence of radial Palmquist cracks, with lengths used to determination the fracture toughness K_Ic, can be seen. Decreasing values of bursting force strength F_P confirm the reduction of adhesion of enamel coats to the steel substrate, conversely from profilographs substantial increase of surface roughness (measured parameters of Ra and Rz are approximately 1,5 times higher in comparison to reference sample) were observed. But it must be stressed that marked difference between samples 2 and 3 was not proved using these methods.

As a result of rotating-ball test was detected the length of the damage region L after 6000 rotations of ball that are marked in Fig. 5 for samples 1, 2 and 3. Resistance to abrasion was sole test, at which the sample 2 exhibits better mechanical properties than sample 3. At Fig. 5 are visible regions of the damage without the circle shape (corresponding to the surface roughness). Their measured lengths L for samples 1, 2, and 3 were estimated to 210 µm, 270 µm, and

Table II
Average values of microhardness, fracture toughness, bursting force by the shot firing test, and surface roughness of the vitreous enamel coat before and after the exposure to indication liquid

	Sample 1 without indication liquids	Sample 2 indication liquid NaCl	Sample 3 indication liquid $NaNO_2$
$HV_{0,1}$ [MPa]	6749,58	7341,39	7450,89
K_{IC} [MPa.m$^{1/2}$]	0,85	0,79	0,80
Bursting force Fp [N]	90	75	80
Surface Roughness [um]	Ra = 0,27 Rz = 1,55	Ra = 0,44 Rz = 2,27	Ra = 0,38 Rz = 2,33

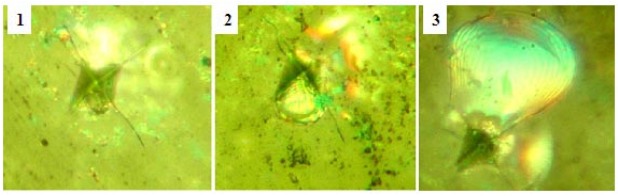

Fig. 4. **Impress of the Hanemann microhardness tester into the surface of enamel coats. Enlarged 1000 times**

300 µm, respectively. In accordance with previous results showing the higher microhardness and lower fracture toughness, the ball test was connected with the crumbling of the particles of the coats, especially for samples 2 and 3. The highes damage was observed for the sample 3 with the higher value of microhardness. It is a typical phenomenon for vitreous enamel coatings.

Results of the scratch test, when the normal force ranges from 40 N to 80 N: The sample 3 exhibits a slow penetration of the indenter into the surface. The scratch was slowly spreading and near the normal loading of 40 N, there was a visible formation of cracks across the scratch. With increasing normal loading, the cracks gradually grew and failures in the surroundings of cracks occurred even at higher normal forces. During acting of the normal force from 0 N to 40 N, the sample 2 showed a similar process, with the difference

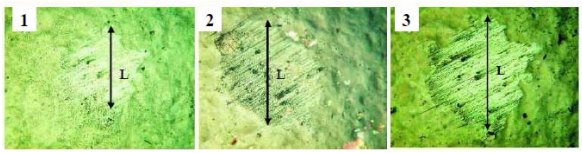

Fig. 5. **Regions of the coat damage with determined damage lengths L after the ball test. Enlarged 100 times**

that cracks were formed at lower normal force. At higher values of normal forces, the most significant failure in the surroundings of the cracks was observed. In contrast, the sample without the exposure of indication liquids (sample 1) embodies the highest resistance and the highest hardening with regard to the width of the scratch. Very shallow cracks are formed at around 40 N. These results were supported by the acoustic emission measurements. We found out that signal courses at all samples have similar character, the first and the latest responses were detected about the forces of 6 N and 12 N in the case of samples 2 and 1, respectively. The graph of static indentation test is shown in Fig. 7. Maximal normal loading of 100 N showed substantial cracking of the sample surface, where the indication fluid with the NaCl content acted (denoted by line with circles). The reference sample (full line) is without distinct failure and the sample with the $NaNO_2$ content (line with square) shows, except small marks at the beginning of the curve and around the values of 35 N and 48 N, gradual increase of small brittle fractures from 78 N of normal loading. The highest depth at nano indentation test (about 4,5 μm) was determined for NaCl enriched sample (see Fig. 8), while at the reference sample 1 and the sample 3 with the $NaNO_2$ content the indenter penetrates into the similar depth of 4,3 μm. 4,4 % difference of penetration depth is a strong influence in the nano-scale. Based on the results of indentation tests we can conclude that indication liquid with NaCl strongly influences surface quality and properties of enamel coatings. These conclusions are supported by the fact that when the samples were unpacked after 3 weeks, surface of the sample 2 observed by optical microscope showed the origin of colour thin plan-parallel layer in the surroundings of the coat fault, which penetrates up to the steel substrate. This layer obviously comes from the reaction of indication liquid with NaCl content and the iron oxides. Note that this phenomenon was not visible at sample 3.

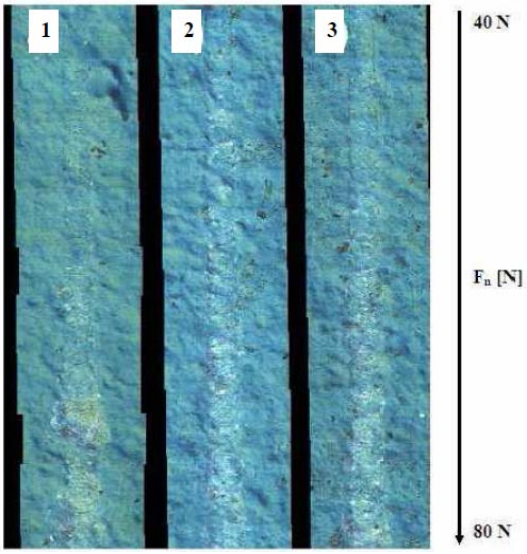

Fig. 6. **Scratch indentation test of vitreous enamel coat before (1) and after (2, 3) exposure to the indication liquid containing NaCl and NaNO2, respectively**

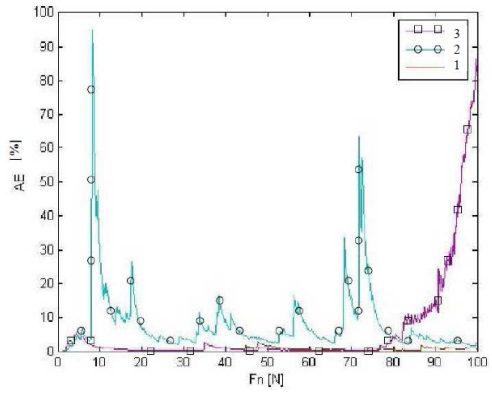

Fig. 7. **Static indentation test – full line and lines with circles and squares correspond to the acoustic emission signals detected from samples 1, 2, and 3, respectively**

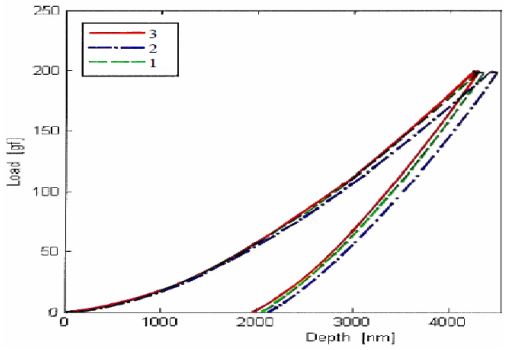

Fig. 8. **Depiction of an indentation curve – dependence of force intensity and deformation during the nano-indentation test with the maximal normal loading of 200 g**

4. Conclusion

Indication liquids are substances used for identifying faults in vitreous enamel coats. Results presented in this paper confirm that their long-time exposure cause the corrosion of vitreous part of enamel coating and in this way significantly decrease final quality of the enamel coat surface. According to these facts, residue of indication liquids after the LVT should be included into the whole process of production monitoring and controlling the quality of vitreous enamel coats at producers. Moreover, mechanical properties of enamel products with deteriorate brittle-fracture parameters often become worse during the transport to the customer.

Acknowledgments – MŠMT ME 08083, MSM6198910016, SP2011/26, CZ.1.05/2.1.00/01.0040.

REFERENCES

1. Podjuklova J.: *Studium vlastností systémem kov-sklovitý smaltový povlak*, VŠB-TUO, 44 (2000).

2. Yatsenko E. A., Ryabova A. V., Zubekhin A. P., Guzii V. A.: Glass Ceram. *54*, 1-2 (1997).
3. Podjuklova J., Mohyla M.: Acta Metall. Slovaca *6*, 380 (2000).
4. Hrabovska K., Barcova K., Podjuklova J., Sionko M.: Acta Mechanica Slovaca *9*, 67 (2005).
5. Yang X., Jha A., Brydson R., Cochrane R. C.: Mater. Sci. Eng. *A366*, 254 (2004).
6. Zhang T., Bao Y., Gawne D. T.: J. Eur. Ceram. Soc. *23*, 1019 (2003).
7. Curtis T.: Shreir's Corrosion, Chapter 3.28, 2330 (2010).
8. Oliver S., Proctor B. A., May C. A.: Shreir's Corrosion *3*, 2306 (2009).
9. Protasova L. G., Kosenko V. G., Farafontova E. P.: Glass Ceram. *60*, 229 (2003).
10. Barcova K., Mashlan M., Zboril R., Filip J., Podjuklova J., Hrabovska K., Schaaf P.: Surf. Coat. Technol. *201*, 1836 (2006).
11. Barcova K., Mashlan M., Zboril R., Hrabovska K.: *AIP Conference proceedings*, (M. Gracia, J.F. Marco, F. Plazaola, ed.). American Institute of Physics 765, 120 (2005).
12. Yang X., Jha A., Brydson R., Cochrane R. C.: *An analysis of the microstructure and interfacial chemistry of steel–enamel interface*. 33–45, (2003).
13. Bouše V.: *Smalty a jejich použití v protikorozní ochraně*, SNTL, Praha 1986.
14. Menčík J.: *Pevnost a lom skla a keramiky*, SNTL, Praha 1990.
15. Hrabovská K., Podjuklová J., Barčová K., Dobrovodská L., Pelikánová K.: Email *4*, 57 (2008).
16. Hrabovská K., Podjuklová J., Pelikánová K., Dobrovodská L., Laník T., Viliamsová J.: Acta Mechanica Slovaca *4 – B*, 126 (2008).
17. Barcova K., Zboril R., Mashlan M., Jiraskova Y., Filip J., Lunacek J., Hrabovska K.: Surf. Interface Anal. *38*, 413 (2006).
18. Hrabovská K., Podjuklová J., Barčová K., Dobrovodská L., Pelikánová K.: Solid State Phenomena *147 -149*, 856 (2009).
19. Dietzel A.: Glass Email *73*, 63 (1940).

K. Hrabovská[a], J. Podjuklová[b], O. Životský[a], K. Barčová[a], I. Štěpánek[c], V. Bártek[b], and T. Laník[b] *([a] Institute of Physics, VŠB-Technical University of Ostrava, Ostrava, [b] Faculty of mechanical Engineering, VŠB-Technical University of Ostrava, Ostrava, [c] Faculty of mechanical Engineering, University of West Bohemia in Pilsen, Plzen, Czech Republic):* **Effect of Indication Liquids on Brittle-Fracture Properties of Vitreous Enamel Coatings**

Vitreous enamel coatings are created by the process of burning at temperature above 800 °C after the application of an enamel slip on metal substrate. To detect the faults and cracks in the coat, which penetrate up to the steel substrate, the coat surface is covered by different types of indication liquids. In this paper we observed the influence of two types of indication liquids on the brittle-fracture of under and top vitreous enamel coatings. Results show that long-time exposure of indication liquids negatively influences brittle-fracture properties. Hence we recommend careful removing of indication liquids from the enamel surface immediately after the low voltage test.

LOCAL STUDIES OF CAST IRON MACHINED SURFACES

ANTONÍN KŘÍŽ

University of West Bohemia, Univerzitní 22, 30614, Plzeň, Czech Republic
kriz@kmm.zcu.cz

Keywords: surface integrity, machined surfaces, special drilling tool, surface morphology

1. Introduction

Chip removal belongs to the machining processes where higher surface quality is required. The surface used to be evaluated to a very limited extent, mostly involving roughness characteristics. Description of surface is more accurate if it includes not only Ra roughness but also additional surface characteristics, in particular the areal roughness. Nowadays, tools, instruments and experience are available that allow better characterization of the state of surface and correlations with resulting properties. Comprehensive examination of machined surfaces is based on state of the art knowledge which is often summarized in the surface integrity concept. The techniques include scratch testing, nanoindentation hardness measurement, cyclic impact testing and local corrosion testing.

1.1. Surface Integrity Concept

Surface integrity exploration is based on the set of instruments at the author's department and on the cooperation with the Department of Machining Technology at the Faculty of Mechanical Engineering of the University of West Bohemia in Plzeň. This cooperation expands to include practical applications thanks to scientific and industrial projects concerning both machining accuracy and the state of surface. Application of surface integrity to practical issues requires a very cautious approach. First, the results obtained are extensive and may not be always relevant to practical use. Second, they might be conflicting. The state of surface used to be described by means of roughness characteristics. Surface and sub-surface defects received some attention as well. In more profound studies, these were even correlated with the material's fatigue behaviour. The comprehensive nature of those results requires that they are treated in an appropriate context and with proper correlations. Measurement of residual stresses may serve as an example[2,4–6]. The problems arise in selection of a method of determining residual stresses with certain (in)accuracy. Others are related to its interpretation and usability in practice. In the real world, problems might occur with the usability of solely residual stress-based findings for rejecting non-conforming products or for predicting service properties. Four years ago, there was only one company on the European market offering defined finishing of machined surfaces, the Baublies AG[1]. Its contribution consists in developing a standalone roller burnishing tool which offered numerous advantages. One of the most important ones is the fact that it is adjustable within a certain range of diameters and this adjustability is useful for worn rollers as well. On the other hand, it also has its drawbacks: the drilled hole must have certain characteristics related not only to accuracy but also surface morphology and hardness. It cannot be used as a combination tool either. Another drawback is its high price which is many times higher than the prices of drills and even broaches. Despite these drawbacks, this company's range of products has no competitor in Europe. This company can boast not only market innovations but also scientific contribution, as it was its product range which introduced the surface integrity concept into engineering practice. Although the American standard on surface integrity, ANSI B211.1 1986, has been presented three years ago, it has been used very little in practice.

This is why broader description of individual properties is necessary. At first sight, these may lead to conflicting findings but in wider context they will be more accurate than mere residual stress measurement whose interpretation is difficult and often impossible. Theoretical aspects of the individual factors of surface integrity are covered in the standard and presented in a number of papers[2–4]. This study aims to describe a specific evaluation of machined surface of drilled holes in a cast iron, focusing both on the resulting accuracy and other surface integrity aspects.

2. Experimental Procedure

This study was aimed at the surface integrity of drilled holes with the depth of 3D where the required tolerance grade was IT6 – IT7. The studied material was gray cast iron. Testing samples were cylinders with the following dimensions: d = 26 mm, l = 36 mm. Three types of drills denoted A, B and C from different companies were used for hole drilling into the cylinders. After drilling, the cylinders were cut along their axis to allow analysis of the machined surface.

The following factors were monitored: surface topography measurement, surface roughness, surface microstructure, microhardness, nanoindentation hardness, scratch, corrosion and impact resistance.

3. Results and Discussion

3.1. Surface Topography

Optical micrographs of surfaces of holes were compared visually and by means of image analysis software.

The surface of the hole drilled with the tool A exhibited dark spots where the machined surface was pulled out during drilling, and light areas where no extraction occurred. Sharp edges of graphite flakes are locations of high stress concentration, contributing to the pull-out of graphite particles or even parts of surface attached to them (see Fig. 1). Analysed surfaces showed parallel markings running at about 30° to the axis of the cylinder, regardless of the tool used. These are

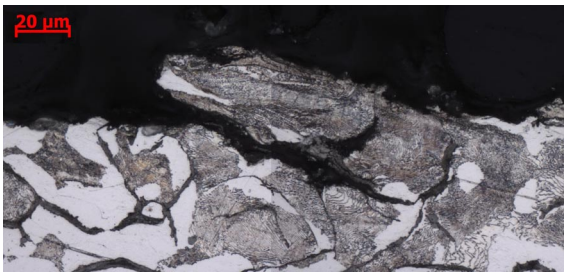

Fig. 1. **Micrography of pull-out of surface in the drilled hole**

probably traces of surface deformation caused by the tool flank while the tool was being removed from the hole. These irregularities can be regarded as undesirable effects impairing the quality of the machined surface. Such surface defects can be detected only using light or scanning confocal microscope, image analysis and measuring areal roughness because they do not affect roughness values. Despite, a number of authors accept roughness values as decisive data for description of surface state. The roughness data cannot be regarded as conclusive, as it does not reflect the actual condition of the surface.

The amount of extracted surface depends on the stress state and on the forces between the tool and machined surface. It is assumed that the higher the internal stress (particularly the tensile stress) in the machined surface, the greater the amount of graphite pulled out together with the matrix by the drilling tool and the greater the depth from which the material is extracted. The quality of the machined surface is impaired by this process. This finding implies that the time-consuming measurement of residual stresses may not be necessary. It is the heterogeneous microstructure of grey cast iron for which this approach proves effective, as the location of material pull-out is governed by the location of graphite under the surface (Fig. 1). The surface relief is affected by the state of microstructure in a definite manner. The study of the surface is useful also for revealing the internal structure which changes in dependence on the introduced stress and temperature. These relations proved true mainly during drilling of D2 tool steel when, with certain machining parameters, the drilled surface re-hardened and its hardness increased markedly again (Fig. 2).

3.2. Surface and Subsurface Microhardness

Microhardness of specimens was measured along two lines located about 50 µm apart and in 50 µm distance from and parallel to the surface. The first line was just beneath the machined surface and in the plastic deformation zone created by the cutting tool. The second line of indentations was in the unaffected material. By comparing average hardnesses along both lines and average standard deviations, one can assess the state of the material surface after machining. Hardness was measured as HV0.015 microhardness.

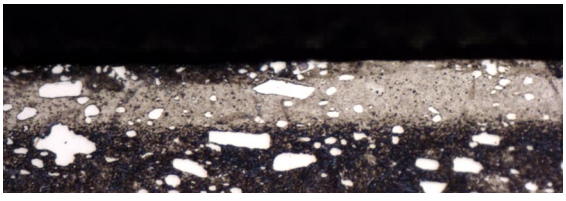

Fig. 2. **Surface hardened to the depth of 30 µm. D2 steel with surface hardness of HV0.01 = 1.107**

The results show that changes in hardness of the material were not consistent. In some cases, hardness of the machined surface decreased, despite the expected influence of plastic deformation. In this case, certain impact of the tool wear cannot be ruled out, as under normal conditions, i.e. normal machining temperature, cast iron should not exhibit softening. The decline may also be explained by the effects of the cutting process, which does not introduce sufficient amount of strain or even lacks the parameters to make the material strengthen above its initial level. The tool A retained its initial parameters throughout the cutting process. The tool B lost its ability to cause work hardening in the material at the end of the drilling process. The tool C with its special geometry caused the material to harden gradually. Compared with C45 steel which was also tested in the present project, the increase in the amount of deformation in cast iron is much smaller.

3.3. Surface and Subsurface Nanohardness

Nanoindentation measurements are carried out in the material unaffected by drilling and in the machined surface. Unlike in the case of conventional microhardness measurement, the effect of hardening was found in all surfaces of drilled holes. The average increase in nanoindentation microhardness HIT in the affected zone was 47 % compared to unaffected material. With the tool A, this increase was 55 %. From the viewpoint of elastic-plastic strain ratio, highest values were found for the tool B: 27.2 %. For the tool C, the elastic-plastic strain ratio was the smallest (24.2 %).

3.4. Scratch Testing

Scratch testing is typically used for assessing the adhesive-cohesive behaviour of thin film-substrate systems. However, it can be employed also fin the case of drilling-affected surface layers. The purpose of measurement was not only to determine the surface hardness but also the surface uniformity along the entire hole depth of 36 mm. Two 18 mm scratches were created on the surface under a constant load of 40 N. Scratch channel volumes were measured using Olympus Lext 3100 confocal microscope at the magnification of 200×.

Volumes of scratch channels on the machined surface of the cast iron show that the largest value (indicating the lowest surface hardness) is associated with the element machined by the tool A. In contrast, the lowest scratch channel volume was found in the element drilled with the tool B. Scratch channel volumes are not very different. The differences are within the measurement error range, which is why these results do not confirm the earlier conclusion that the tool A produces the softest surface.

Results of this analysis have been included in this paper on purpose, although they do not correspond to the above findings and are in contradiction to the assumption that

scratch channels are less deep in materials with higher hardness. This contradiction illustrates the difficulties inherent to characterising comprehensive properties of real-world surfaces in relation to surface integrity.

3.5. Corrosion Resistance Tests

The purpose of the corrosion test was to assess the impact of the state of machined surface on the corrosion behaviour. This simple corrosion test does not clearly indicate if the dominant aspect is the surface topography or the activation energy increased by plastic deformation. The most rapid corrosion was seen in specimens drilled with the tool B. The other drilled holes showed very similar results. After finding additional correlations, it was shown that the surface created by the tool B contains more defects, pull-out regions and higher hardness. In this case, the surface relief proved more significant than the plastic strain introduced, as the latter was negligible in the machined surfaces.

3.6. Cyclic Impact Test

Impact resistance of hole surfaces was evaluated by means of the cyclic impact test. It consists in cyclic impact loading of the surface. The blows are repeated with certain pre-defined frequency and energy.

The examined surfaces were subjected to identical loads consisting in 5,000 impacts with the lowest energy available in the setup. The purpose of the test was to measure the properties of those surface areas where different effects of the cutting tools were expected. The test created an impact crater which was then examined. The crater dimensions were measured and characteristics of degradation processes were determined (surface layer delamination, cracks).

The craters were observed in a light microscope and using a scanning electron microscope (SEM).

The dimensions of craters did not differ significantly. It is due to the fact that the state of machined surfaces does not vary enough under the presently used impact test conditions to be detected. SEM examination of defects in the crater revealed that the surface machined with the tool C was of higher quality than those created by the other two tools. Thus, a surface machined with high-quality tools has negligible influence on degradation processes under impact loads in ordinary service. Detecting the state of machined surfaces more accurately would require much lower energy of the impact body than in the current test.

4. Conclusions

The concept of surface integrity encompasses various methods to obtain comprehensive image of the state of machined surface. Unfortunately, some results can be conflicting and difficult to classify without contradictions. This may be due to lack of accuracy of measurement but one cannot exclude effects of unknown factors which have different impact in different types of measurement. The former cause can be eliminated by larger number of measurements and by statistical processing of results, taking account of the standard deviation. The latter causes are difficult to identify. They can only be eliminated through better understanding of undergoing processes. This applies to, for instance, the corrosion tests where the results depend on competing effects. Despite these difficulties, surface integrity data are valuable for academic but also for practical applications. In this case, it applies to evaluation of surfaces created by specially designed "finishing" drills. The surface integrity concept will be further developed based on the collaboration of the academic sphere and manufacturers and users of cutting tools.

This paper is one of the outcomes of the project No. FI-IM4/226, which is co-funded by the Ministry of Industry and Trade of the Czech Republic and the company HOFMEISTER s.r.o.

REFERENCES

1. Website of the company Baublies AG available online at: http://www.baublies.com/de/index.html, accessed 2 Aug 2010.
2. Kříž A., Šimeček J.: *Conference proceedings of Vrstvy a Povlaky, Rožnov pod Radhoštěm, 2009.* LISS a.s., 2009, pp. 36-42.
3. Kříž A.: Integrita povrchu a její význam v praktickém použití. Available on-line at: http://www.ateam.zcu.cz, accessed 2 Dec 2009.
4. Kříž A., Šimeček J.: *Conference proceedings of Tepelné zpracování. Jihlava, 2009.* Ecosond, 2009, pp. 1-6.
5. Bumbálek B.: Integrita povrchu a její význam pro posouzení vhodnosti dané plochy pro její funkci. Online at http://www.ateam.zcu.cz, accessed 2 Dec 2009.
6. Stephenson D. J.: Surface Integrity Control During The Precision Machining Of Brittle Materials, available online at http://www.azom.com, accessed 2 Dec 2009.

A. Kříž *(University of West Bohemia, Plzeň, Czech Republic):* **Local Studies of Cast Iron Machined Surfaces**

The surface integrity concept represents a comprehensive characterization of all influences affecting the surface properties and the end-use properties of a product.

This paper describes practical application of the concept of surface integrity to holes drilled in gray cast iron with special tools.